British Journal of Pharmacology

DOI:10.1111/j.1476-5381.2012.02040.x
www.brjpharmacol.org

RESEARCH PAPER

Toll-like receptor 4 knockout protects against anthrax lethal toxin-induced cardiac contractile dysfunction: role of autophagy

Machender R Kandadi[1], Arthur E Frankel[2] and Jun Ren[1]

[1]*Center for Cardiovascular Research and Alternative Medicine, University of Wyoming, College of Health Sciences, Laramie, WY, USA, and* [2]*Cancer Research Institute of Scott & White Memorial Hospital, Temple, TX, USA*

Correspondence
Jun Ren, Center for Cardiovascular Research and Alternative Medicine, University of Wyoming, College of Health Sciences, Laramie, WY 82071, USA. E-mail: jren@uwyo.edu

Keywords
anthrax; lethal toxin; cardiac function; intracellular Ca^{2+}; ER stress; autophagy

Received
19 October 2011
Revised
13 April 2012
Accepted
24 April 2012

BACKGROUND AND PURPOSE

Anthrax lethal toxin (LeTx) is known to induce circulatory shock and death, although the underlying mechanisms have not been elucidated. This study was designed to evaluate the role of toll-like receptor 4 (TLR4) in anthrax lethal toxin-induced cardiac contractile dysfunction.

EXPERIMENTAL APPROACH

Wild-type (WT) and TLR4 knockout ($TLR^{-/-}$) mice were challenged with lethal toxin (2 $\mu g \cdot g^{-1}$, i.p.), and cardiac function was assessed 18 h later using echocardiography and edge detection. Small interfering RNA (siRNA) was employed to knockdown TLR4 receptor or class III PI3K in H9C2 myoblasts. GFP–LC3 puncta was used to assess autophagosome formation. Western blot analysis was performed to evaluate autophagy (LC3, Becline-1, Agt5 and Agt7) and endoplasmic reticulum (ER) stress (BiP, eIF2α and calreticulin).

KEY RESULTS

In WT mice, lethal toxin exposure induced cardiac contractile dysfunction, as evidenced by reduced fractional shortening, peak shortening, maximal velocity of shortening/re-lengthening, prolonged re-lengthening duration and intracellular Ca^{2+} derangement. These effects were significantly attenuated or absent in the TLR4 knockout mice. In addition, lethal toxin elicited autophagy in the absence of change in ER stress. Knockdown of TLR4 or class III PI3 kinase using siRNA but not the autophagy inhibitor 3-methyladenine significantly attenuated or inhibited lethal toxin-induced autophagy in H9C2 cells.

CONCLUSION AND IMPLICATIONS

Our results suggest that TLR4 may be pivotal in mediating the lethal cardiac toxicity induced by anthrax possibly through induction of autophagy. These findings suggest that compounds that negatively modulate TLR4 signalling and autophagy could be used to treat anthrax infection-induced cardiovascular complications.

Abbreviations

EF, oedema factor; $\pm dL/dt$, maximal velocity of shortening/re-lengthening; 3-MA, 3-methyladenine; LeTx, anthrax lethal toxin; LF, lethal factor; PLN, phospholamban; PA, protective antigen; PS, peak shortening; SERCA, sarco(endo)plasmic reticulum Ca^{2+}-ATPase; TLR4, toll-like receptor 4; TPS, time to 90% peak shortening; TR_{90}, time to 90% re-lengthening

Introduction

Bacillus anthracis, a spore-forming, Gram-positive bacterium, is the known causative factor for anthrax. Anthrax infection is highly lethal and represents a major bioterrorism threat. Infection through inhalation of *B. anthracis* spores may trigger a high mortality rate of up to 80% (Borio *et al.*, 2001; Fraser and Dando, 2001). Major routes of infection are mediated through inhalation, cutaneous or ingestion of *B. anthracis* spores. Individuals with anthrax exposure have often been found to develop refractory hypotension unresponsive to the standard antibiotics, fluid, pressor and respiratory support (Barakat *et al.*, 2002). Anthrax toxin is believed to be the major virulence factor of *B. anthracis*, consisting of three polypeptides namely oedema factor (EF), lethal factor (LF) and protective antigen (PA). The combination of LF and the receptor binding PA forms the highly toxic lethal toxin (LeTx) (Moayeri *et al.*, 2004). LF is a zinc metalloprotease that cleaves the NH_2-terminal of MAPK kinases (MEKs) resulting in inactivation of the kinase. EF is a calmodulin-dependent AC, which promotes intracellular cAMP accumulation and associated cellular responses (Cui *et al.*, 2004; Rossi *et al.*, 2008; Moayeri and Leppla, 2009). PA binds cellular receptors tumour endothelial marker 8 (TEM8) and capillary morphogenesis gene 2 (CMG2) (Bradley *et al.*, 2001; Scobie *et al.*, 2003). Once bound to the receptor and proteolytically activated, PA forms a heptamer that delivers EF and/or LF to the cytoplasm following receptor-mediated endocytosis. Although lethal toxin has been reported to compromise cardiac function (Watson *et al.*, 2007a; 2007b; Kuo *et al.*, 2008; Moayeri *et al.*, 2009), the precise molecular mechanisms underlying lethal toxin-mediated detrimental effects on the heart remain unclear.

Autophagy is a regulated process through which mammalian cells degrade and recycle macromolecules and organelles. Under physiological conditions, autophagy plays a vital role in a wide array of cellular responses including maintenance of amino acid pool during starvation, suppression of neurodegeneration, aging and tumour genesis as well as clearance of intracellular microbes. Autophagy can be activated by pathophysiological stress stimuli such as hypoxia, energy depletion and endoplasmic reticulum (ER) stress, bacterial, viral and parasite infections. Although multiple molecular machineries have been reported to induce autophagy (Kroemer *et al.*, 2010), ER stress is one of the major stimulators of the autophagic response that participates in the degradation of unfolded proteins and removal of superfluous ER membranes under pathological conditions (Yorimitsu *et al.*, 2006). ER function is usually involved in the correction of protein folding and post-translational modification, although excessive stress may trigger autophagy due to inadequate compensatory mechanisms.

It was suggested that mice deficient in toll-like receptor (TLR)-4 are resistant to anthrax exposure-induced toxicity (Hughes *et al.*, 2005). Likewise, macrophages from TLR4-deficient mice display reduced apoptosis in response to *B. anthracis* infection (Hsu *et al.*, 2004). These findings indicate a possible role for TLR4 in anthrax-induced cytotoxicity. TLRs are a family of receptors capable of recognizing pathogen-associated molecular moieties shared by a large group of microorganisms, thereby assisting in microbial recognition by host immune systems. To-date, several different TLRs have been identified with the ability to distinguish a variety of microbial conserved patterns (Takeda and Akira, 2005), including the main constituents of the Gram-negative and the Gram-positive bacteria (Poltorak *et al.*, 1998; Schwandner *et al.*, 1999), among which TLR-4 is activated by bacterial LPS to facilitate the NF-κB-dependent expression of pro-inflammatory cytokines, such as TNF-α and IL-1β (Baumgarten *et al.*, 2001). In an effort to better understand lethal toxin-induced cardiac contractile dysfunction, we examined the role of TLR4 in anthrax lethal toxin-induced cardiac contractile and intracellular Ca^{2+} responses as well as the underlying mechanisms involved, with a particular focus on autophagy.

Methods

Experimental animals and anthrax lethal toxin challenge

All studies involving animals are reported in accordance with the ARRIVE guidelines (Kilkenny *et al.*, 2010; McGrath *et al.*, 2010). All animal procedures described in this study were approved by the Animal Care and Use Committee at the University of Wyoming (Laramie, WY). Animals were housed under well-controlled conditions of temperature (22 ± 2°C), humidity (55 ± 5%) and a 12 h/12 h light–dark cycle with access to food and water *ad libitum*. $TLR4^{-/-}$ (TLR4 knockout) and $TLR4^{+/+}$ (wild-type C57BL/6J) mice were purchased from the Jackson Laboratories (Bar Harbor, ME); the total number of mice used was 30. Four-month-old adult male $TLR4^{-/-}$ and their age-matched wild-type control mice were injected i.p. with anthrax lethal toxin (2 $\mu g \cdot g^{-1}$, LF + PA 1:2 ratio) and were killed under anaesthesia (ketamine/xylazine: 3:1, 1.32 $mg \cdot kg^{-1}$, i.p.) 18 h later. Recombinant PA and LF were produced and purified as previously described (Watson *et al.*, 2007a; 2007b; Kandadi *et al.*, 2010). The toxins were stored at –80°C in PBS with a pH of 7.4. Immediately prior to injection, toxin components were thawed and mixed in PBS.

Echocardiographic assessment

Cardiac geometry and function were evaluated in anaesthetized (Avertin 2.5%, 10 $\mu L \cdot g^{-1}$ body weight) mice by use of two-dimensional guided M-mode echocardiography with a Sonos 5500 (Philips Medical Systems, Andover, MA, USA) equipped with a 15 to 16 MHz linear transducer. Left ventricular anterior and posterior wall dimensions during diastole and systole were recorded from three consecutive cycles in M mode by methods adopted by the American Society of Echocardiography. Fractional shortening was calculated from LV end-diastolic (EDD) and end-systolic (ESD) diameters with the equation (EDD – ESD)/EDD × 100. Cardiac output was calculated from LV end-diastolic and end-systolic diameters using the equation $[(LVEDD)^3 - (LVESD)^3] \times$ heart rate. Heart rates were averaged over 10 cardiac cycles (Gardin *et al.*, 1995).

Cardiomyocyte isolation

After ketamine/xylazine sedation, hearts were removed and perfused with Krebs–Henseleit buffer containing (in mmol L^{-1}): 118 NaCl, 4.7 KCl, 1.2 $MgSO_4$, 1.2 KH_2PO_4, 25 $NaHCO_3$,

10 HEPES and 11.1 glucose. Hearts were digested with 223 U·mL^{-1} collagenase D for 20 min. Left ventricles were removed and minced before being filtered. Myocyte yield was ~75%, which was not affected by either acute lethal toxin challenge or TLR4 knockout. Only rod-shaped myocytes with clear edges were selected for mechanical study (Relling *et al.*, 2003).

Cell shortening and re-lengthening

Mechanical properties of cardiomyocytes were evaluated utilizing a SoftEdge MyoCam system (IonOptix Corporation, Milton, MA) (Ceylan-Isik *et al.*, 2009). Briefly, cardiomyocytes were visualized under an inverted microscope (Olympus, IX-70, Olympus Optical Co., Tokyo, Japan) and were stimulated with a frequency of 0.5 Hz. The myocyte being observed was shown on a computer monitor using an IonOptix MyoCam camera. IonOptix SoftEdge software was utilized to capture cell shortening and re-lengthening changes. The indices being examined included peak shortening amplitude, time to peak shortening (TPS), time to 90% re-lengthening (TR_{90}) and maximal velocity of shortening/re-lengthening (±dL/dt).

Intracellular Ca^{2+} transients

Isolated cardiomyocytes were loaded with fura-2/AM (0.5 μmol·L^{-1}) for 10 min, and fluorescence intensity was recorded with a dual-excitation fluorescence photomultiplier system (IonOptix). Myocytes were placed onto an Olympus IX-70 inverted microscope and imaged through a Fluor 40× oil objective. Cells were exposed to light emitted by a 75 W lamp and passed through either a 360 or a 380 nm filter while being stimulated to contract at 0.5 Hz. Fluorescence emissions were detected between 480 and 520 nm, and qualitative change in fura-2 fluorescence intensity was inferred from the fura-2 fluorescence intensity ratio at the two wavelengths (360/380). Fluorescence decay time was calculated as an indicator of intracellular Ca^{2+} clearance (Hintz *et al.*, 2003).

Cell culture and treatment

H9C2 cells, a clonal cell line derived from fetal rat heart, were purchased from American Type Culture Collection (ATCC, Manassas, VA). Cells were grown in DMEM supplemented with 10% FBS (Gibco, Grand Island, NY) and 1% penicillin and streptomycin and maintained in 95% air and 5% CO_2 at 37°C. Cells were grown to 80% confluence before being exposed to anthrax lethal toxin.

RNA interference

Small interfering RNA (siRNA) against TLR4 receptor and PI3K class III (On-TARGET plus SMART pool siRNA) or a non-targeting sequence was purchased from Dharmacon (Lafayette, CO, USA). The H9C2 cell cultures were transfected with siRNA (20 nM) in DMEM medium using the transfection reagent (DharmaFECT 1) following the manufacturer's instructions. Seventy two h later, cells were subjected to anthrax lethal toxin exposure (100 ng·mL^{-1} for 3 h).

LC3B–GFP–adenovirus production and infection

Adenovirus containing the LC3-GFP construct was a kind gift from Dr Cindy Miranti (Van Andel Institute, Grand Rapids, MI) and was propagated using the HEK293 cell line. Briefly, cells were infected with LC3-GFP adenovirus; and upon plaque formation, infected cells were collected, washed with PBS, re-suspended in culture medium and lysed by three cycles of freezing (dry ice)–thawing (37°C). Cell debris was collected by centrifugation, and aliquots of supernatant with viral particles were stored at –80°C. Adenovirus was purified using an Adeno-X Maxi purification kit from Clontech (Clontech Laboratories, Inc. Mountain View, CA). H9C2 cells were grown to confluence on Lab-Tek chamber slide. Cells were then infected at an MOI of 2 with adenoviruses expressing LC3–GFP fusion protein. Medium was replaced with fresh DMEM after 6 h. Twenty four h later, cells were visualized for autophagy using confocal microscopy (Edick *et al.*, 2007).

Quantification of the GFP-LC3

H9C2 cells transfected with GFP-LC3 adenovirus were treated with or without anthrax lethal toxin (100 ng·mL^{-1} for 3 h). The cells were fixed with 4% paraformaldehyde in PBS for 20 min at room temperature. Cells were then washed with PBS three times. These fixed cells were treated with DAPI for 5 min followed by three washes with PBS. Coverslips were mounted on the slides using Vecta Mount™ AQ-aqueous mounting medium (Vector Laboratories, Inc, Burlingame, CA). For analysis of autophagy, cells were visualized at 40× magnification using a Zeiss LSM 710 confocal microscope (Carl Zeiss MicroImaging GmbH, Jena, Germany), and the percentage of cells displaying sufficient GFP-LC3 puncta (>10 dots per cell) were scored as autophagy positive as described previously (Edick *et al.*, 2007). A minimum of 75–100 cells were examined for each condition from at least three independent experiments.

Western blotting

Protein samples for Western blotting were prepared as described previously (Dong *et al.*, 2005; Kandadi *et al.*, 2010). Briefly, ventricular tissues or H9C2 cells were homogenized and sonicated in a lysis buffer containing 20 mmol·L^{-1} Tris (pH 7.4), 150 mmol·L^{-1} NaCl, 1 mmol·L^{-1} EDTA, 1 mmol·L^{-1} EGTA, 1% Triton, 0.1% SDS and 1% protease inhibitor cocktail. Equal amounts (50 μg) of proteins were separated on 7%, 10%, 12% or 15% SDS-polyacrylamide gels in a minigel apparatus (Mini-PROTEAN II, Bio-Rad Laboratories Inc., Hercules, CA) and were then transferred electrophoretically to nitrocellulose membranes. The membranes were blocked with 5% milk in Tris-buffered saline before overnight incubation at 4°C with anti-Beclin-1 (1:1000), anti-Atg5(1:1000), anti-Atg7 (1:1000), anti-LC3 (1:1000), anti-BiP (1:1000), anti-phosphorylated eIF2α (peIF2α, Ser^{51}, 1:1000), anti-eIF2α (1:1000), anti-calreticulin (1:1000), anti-TLR4 (1:1000), anti-TRAF6 (1:1000), anti-phosphorylated phospholamban (pPLN, Ser^{16}, 1:1000), anti-PLN (1:1000), anti-SERCA2 (1:1000) and anti-GAPDH (1:1000) antibodies. Membranes were then incubated for 1 h with HRP-conjugated secondary antibody (1:5000).

Statistical analysis

Data are expressed as mean ± SEM. Statistical significance ($P < 0.05$) for each variable was estimated by ANOVA followed by Tukey's test for *post hoc* analysis.

Results

General and echocardiographic properties of WT and TLR4$^{-/-}$ mice with or without lethal toxin challenge

Short-term lethal toxin challenge did not induce any mortality within 18 h in either WT or TLR4 knockout group. Lethal toxin treatment did not affect body and organ weights (heart, liver, kidney and spleen) or organ size (organ weight normalized to body weight) in either WT or TLR4 knockout mice. TLR4 knockout itself did not affect body and organ weights or organ size. Echocardiographic measurements revealed that heart rate, wall thickness and LV end-systolic diameter (LVESD) were comparable among all groups. Lethal toxin significantly decreased LV end-diastolic diameter (LVEDD), fractional shortening and cardiac output in WT mice. In contrast, these effects were not seen in TLR4 knockout mice. TLR4 knockout did not significantly affect the echocardiographic indices tested (Table 1). These findings reveal a beneficial role of TLR4 knockout against lethal toxin-induced cardiac functional changes.

Effect of anthrax lethal toxin on cardiomyocyte mechanics in WT and TLR4$^{-/-}$ mice

Resting cell length was comparable in cardiomyocytes from WT and TLR4$^{-/-}$ mice with or without lethal toxin treatment. Short-term lethal toxin challenge significantly reduced PS, $\pm$dL/dt and prolonged TR_{90} without affecting TPS. Interestingly, TLR4 knockout abolished lethal toxin-induced mechanical abnormalities without eliciting any mechanical effect itself (Figure 1). To explore the possible mechanism of action behind lethal toxin-induced mechanical abnormalities, intracellular Ca^{2+} handling was evaluated using fura-2 fluorescence microscopy in cardiomyocytes from WT and TLR4$^{-/-}$ mice. The results depicted in Figure 2 show that a significant decrease in both basal and electrically-stimulated rise in intracellular Ca^{2+} levels associated with prolonged intracellular Ca^{2+} decay rate followed lethal toxin challenge; these effects were not observed in the TLR4 knockout mice. TLR4 knockout itself did not affect the intracellular Ca^{2+} properties tested.

Effect of TLR4 receptor knockout or knockdown on lethal toxin-induced autophagy

To explore the possible role of autophagy in lethal toxin-induced cardiac mechanical and intracellular Ca^{2+} anomalies, protein markers of autophagy were examined in WT and TLR4$^{-/-}$ mouse hearts with or without lethal toxin exposure. Our data shown in Figure 3A–D revealed a significant elevation in LC3-II levels without any change in the expression of Beclin-1 and Atg7 following lethal toxin challenge; no increase in LC3-II levels was observed in TLR4 knockout mice. TLR4 knockout itself did not affect the autophagy markers tested. To further confirm the role of TLR4 in lethal toxin-induced autophagy induction, the H9C2 myoblasts were transfected with a siRNA against TLR4. Cells were then subjected to lethal toxin exposure before assessment of autophagy. Our results, shown in Figure 3E,F, indicate that knockdown of TLR4 with specific siRNA prevented lethal toxin-induced induction of autophagy. These results provide direct evidence for a role of TLR4 in lethal toxin-induced autophagy.

Table 1

Biometric and echocardiographic parameters in mice challenged with or without LeTx

Parameter	WT	WT-LeTx	TLR4$^{-/-}$	TLR4$^{-/-}$ – LeTx
Body weight (g)	28.1 ± 1.5	28.6 ± 1.7	28.5 ± 1.1	26.9 ± 1.0
Heart weight (mg)	171 ± 18	178 ± 6	162 ± 16	150 ± 12
Heart weight/bodyweight (mg·g^{-1})	6.13 ± 0.53	6.15 ± 0.41	5.74 ± 0.62	5.66 ± 0.59
Liver weight (g)	1.30 ± 0.07	1.20 ± 0.08	1.34 ± 0.05	1.18 ± 0.05
Liver weight/body weight (mg·g^{-1})	46.5 ± 1.1	42.3 ± 2.5	47.0 ± 1.3	44.1 ± 2.3
Kidney weight (mg)	350 ± 24	401 ± 19	362 ± 29	323 ± 23
Kidney weight/body weight (mg·g^{-1})	12.8 ± 0.8	14.4 ± 1.3	12.9 ± 1.2	12.1 ± 1.1
Spleen weight (mg)	74 ± 4	79 ± 4	71 ± 7	65 ± 4
Spleen weight/body weight (mg·g^{-1})	2.66 ± 0.12	2.80 ± 0.21	2.50 ± 0.27	2.47 ± 0.15
Heart rate (beats min^{-1})	435 ± 19	445 ± 12	394 ± 15	371 ± 10
Wall thickness (mm)	0.89 ± 0.03	0.80 ± 0.06	0.80 ± 0.05	0.79 ± 0.06
LVEDD (mm)	2.49 ± 0.11	2.08 ± 0.16*	2.66 ± 0.10	2.40 ± 0.11$^{\#}$
LVESD (mm)	1.23 ± 0.07	1.27 ± 0.08	1.30 ± 0.05	1.29 ± 0.12
Fractional shortening (%)	52.3 ± 1.9	37.6 ± 3.4*	51.4 ± 1.5	46.5 ± 4.1$^{\#}$
Cardiac output (mm^3·min^{-1})	4912 ± 364	2488 ± 419*	5926 ± 461	4381 ± 610$^{\#}$

Mean ± SEM, n = 8–10 mice per group, *P < 0.05 versus WT group; $^{\#}P$ < 0.05 versus WT-LeTx group.

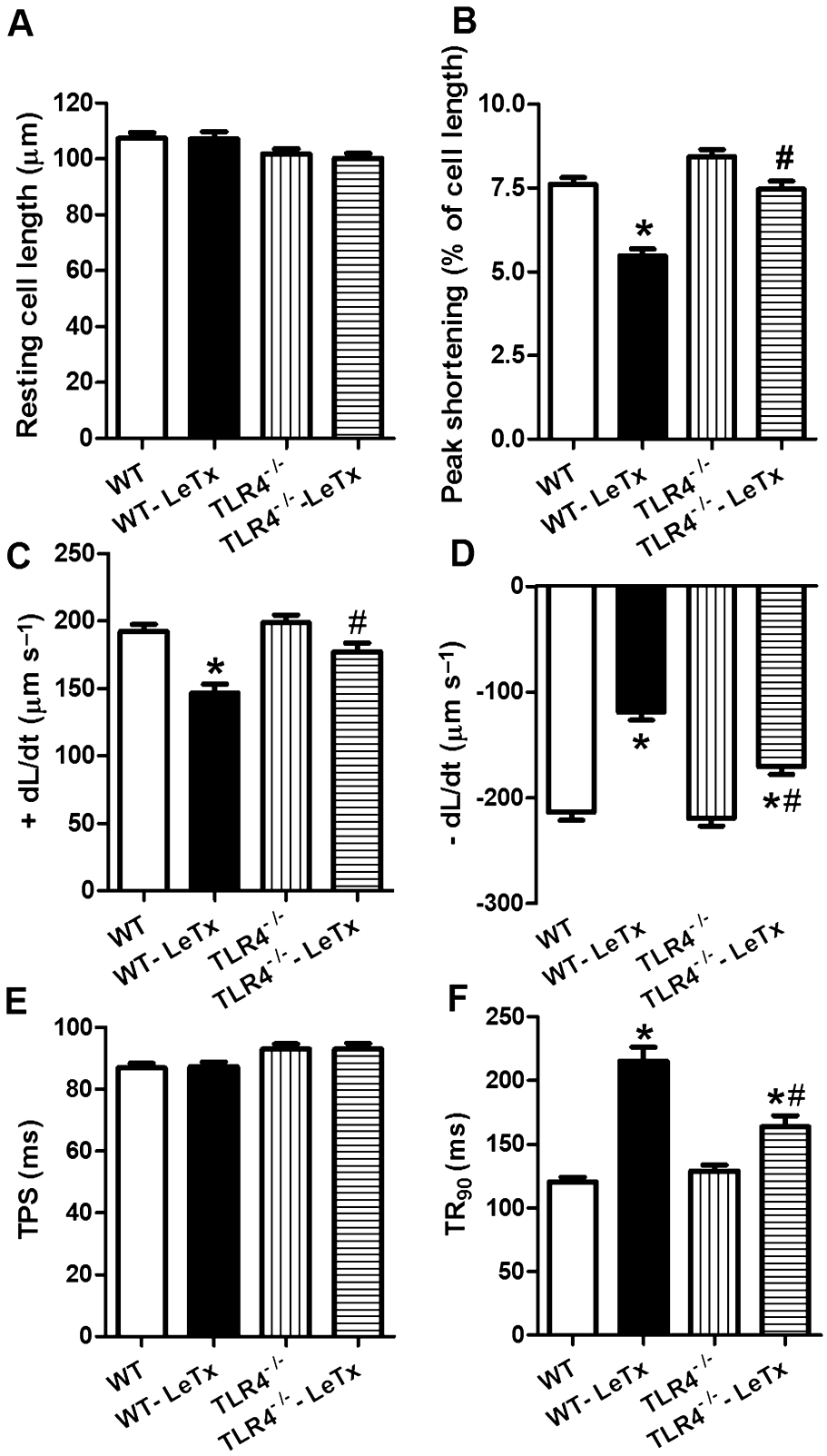

Figure 1

Effect of LeTx (2 μg·g^{-1}, i.p., 18 h) on cardiomyocyte shortening from WT and TLR4$^{-/-}$ mice. (A) Resting cell length. (B) PS (normalized to resting cell length). (C) +d*L*/d*t*. (D) –d*L*/d*t*. (E) TPS. (F) TR_{90}. Mean ± SEM, n = 120 to 150 cells from three mice per group, *P < 0.05 versus WT group, #P < 0.05 versus WT-LeTx group.

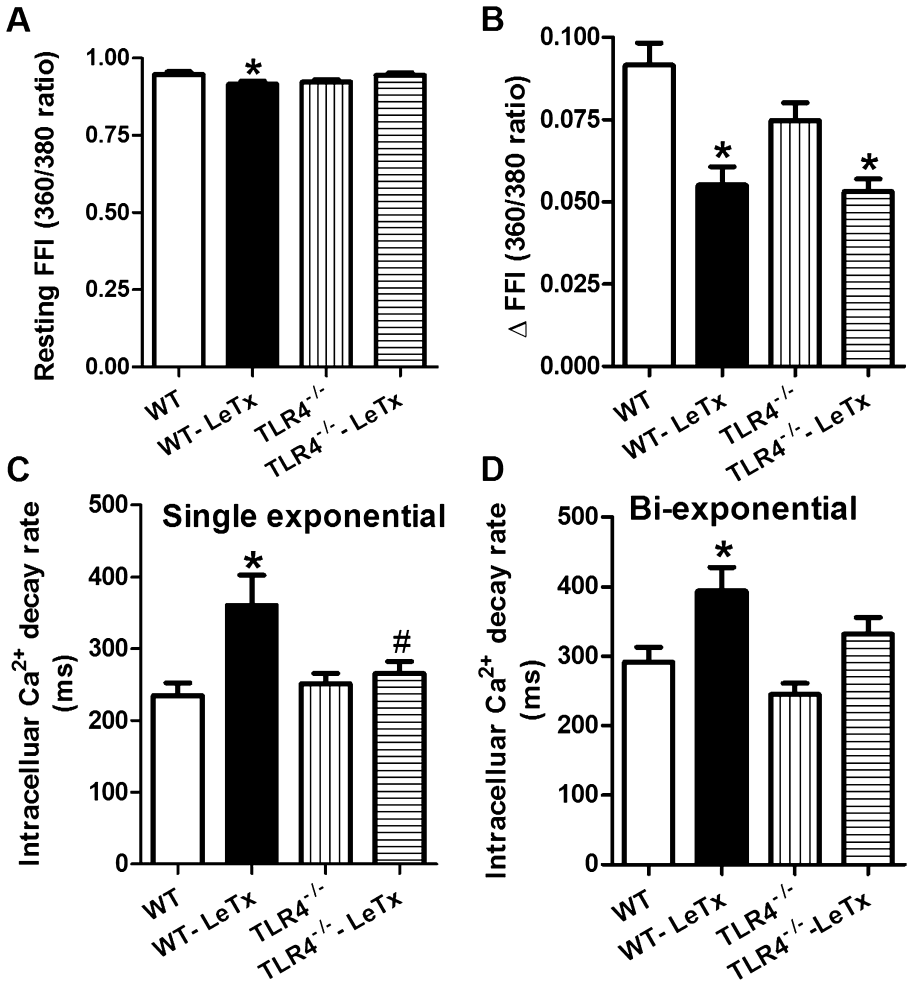

Figure 2

Effect of LeTx (2 μg·g^{-1}, i.p., 18 h) on intracellular Ca^{2+} homeostasis in cardiomyocytes from WT and TLR4$^{-/-}$ mice. (A) Resting fura-2 fluorescence intensity (FFI). (B) Electrically-stimulated rise in FFI (ΔFFI). (C) Intracellular Ca^{2+} transient decay rate (single-exponential). (D) Intracellular Ca^{2+} transient decay rate (bi-exponential). Mean ± SEM, n = 60–75 cells from three mice per group, *P < 0.05 versus WT group, #P < 0.05 versus WT-LeTx group.

Effect of TLR4 knockout and lethal toxin on intracellular Ca^{2+} regulatory proteins

To further understand the mechanisms responsible for lethal toxin-induced intracellular Ca^{2+} mishandling, the expression of the key intracellular Ca^{2+} regulatory proteins was examined in hearts from WT and TLR4$^{-/-}$ mice. Our results, shown in Figure 4, reveal that neither short-term lethal toxin exposure nor TLR4 knockout overtly affected the levels of SERCA2a and the SERCA inhibitory protein phospholamban. In addition, phosphorylation of phospholamban was not altered by either lethal toxin exposure or TLR4 knockout.

Lethal toxin induces autophagy in H9C2 myoblasts

To examine the possible mechanism(s) involved in lethal toxin exposure-induced cardiac anomalies, autophagy was examined in H9C2 myoblasts using immunofluorescence. To detect autophagosome formation, green fluorescent protein fused with LC3 (GFP–LC3) was used as the surrogate marker. LC3 exists in two isoforms, a 16 kDa cytosolic form (LC3-I) and a 14 kDa processed form (LC3-II), which are localized on the autophagosome membrane where they play a pivotal role in autophagosome enlargement (Kabeya *et al.*, 2000). On the initiation of autophagy, GFP–LC3-I is processed to GFP–LC3-II before being recruited onto the autophagosome membrane and can be viewed as punctuate through a fluorescence microscope. H9C2 myoblasts were infected with GFP–LC3 before being exposed to the lethal toxin (100 ng·mL^{-1} for 3 h). Our data revealed that lethal toxin elicited autophagosome formation in approximately 26% cells compared with <2% in control cells. Along the same line, lethal toxin significantly increased levels of Beclin-1 and the LC3-II-to-LC3-I ratio without affecting the expression of Agt5 and Agt7 (Figure 5).

To further understand the mechanism involved in lethal toxin-induced autophagy, H9C2 myoblasts were pre-treated with the lysosomal protease inhibitor pepstatin A (10 μg·mL^{-1}, 1 h) to block autophagolysosome formation and

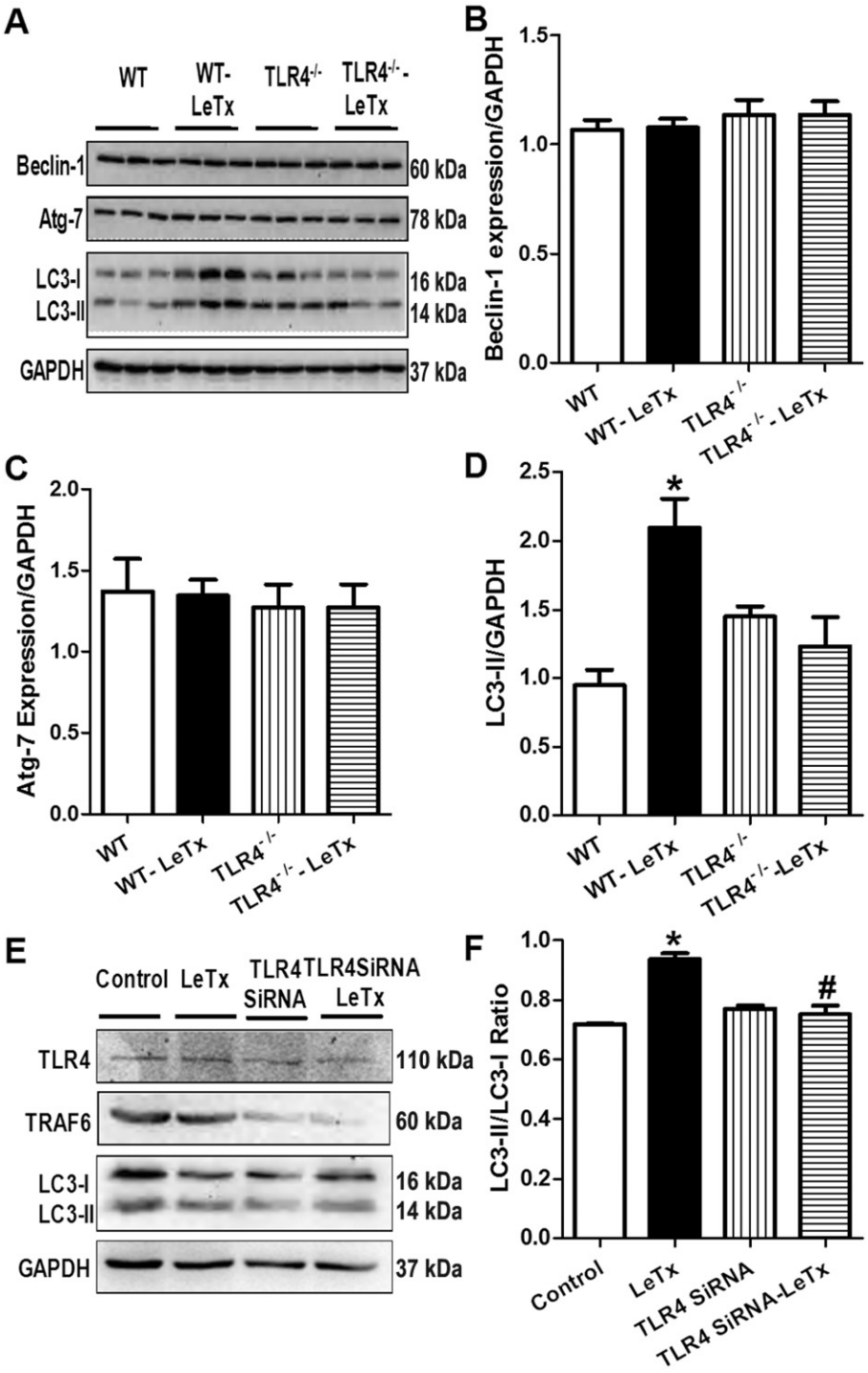

Figure 3

Effect of TLR4 knockout or knockdown on LeTx-induced autophagy. (A) Representative gel blots depicting expression of Beclin-1, Atg7, LC3-I/II and GAPDH (loading control) in LeTx-treated WT and TLR4$^{-/-}$ mouse hearts. (B) Beclin-1. (C) Atg7. (D) LC3-II. (E) Representative gel blots of TLR4, TRAF6, LC3 and GAPDH (loading control) in control and LeTx (100 ng·mL^{-1} for 3 h)-treated H9C2 cells transfected with or without TLR4 siRNA. (F) Pooled data of LC3-II/I ratio in control and LeTx-treated H9C2 cells transfected with or without TLR4 siRNA. Mean ± SEM, n = 4 mice or independent cultures per group, *P < 0.05 versus WT or control group, #P < 0.05 versus LeTx group.

LC3-II degradation in autophagosomes (Tanida *et al.*, 2005). The lethal toxin-induced increases in the LC3-II-to-LC3-I ratio and GFP–LC3^{+} puncta were significantly augmented in the presence of pepstatin A although pepstatin A itself failed to affect the LC3-II-to-LC3-I ratio and GFP–LC3^{+} puncta (Figure 6). These data suggest a possible involvement of autophagic flux in lethal toxin challenge-triggered autophagy response.

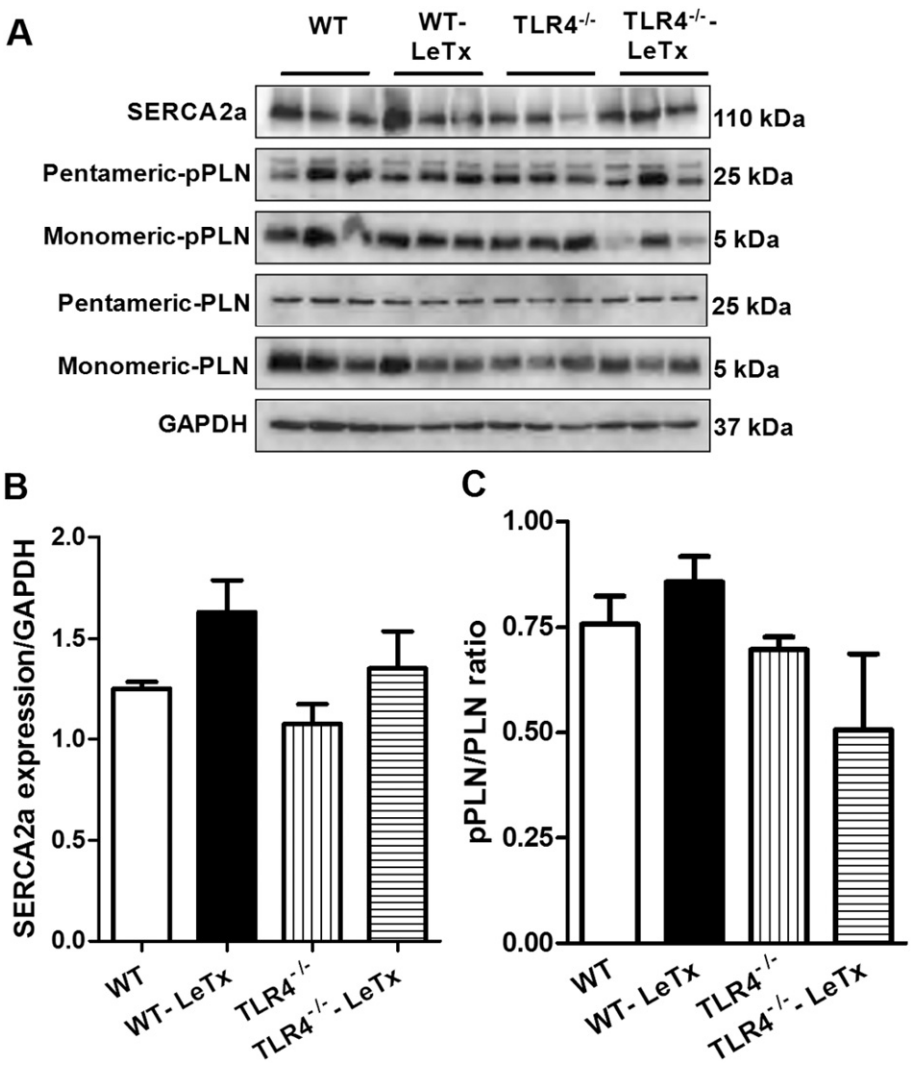

Figure 4

Effect of TLR4 knockout on LeTx (2 μg·g^{-1}, i.p., 18 h)-induced changes in intracellular Ca^{2+} regulatory proteins in WT and TLR4$^{-/-}$ mouse heart. (A) Representative gel bots depicting expression of SERCA2a, pan and phosphorylated phospholamban (Ser^{16}) (PLN, 5 kDa and 25 kDa) and GAPDH (loading control). (B) SERCA2a. (C) Phosphorylated PLN (pPLN)-to-PLN ratio. Mean ± SEM, n = 6 mice per group.

Chemical inhibition of class III PI3K or PI3K knockdown on lethal toxin-induced autophagy

Class III PI3K is known to be involved in the initial step of autophagosome formation. The classic PI3K inhibitors 3-methyladenine (3-MA) and wortmannin inhibit autophagy (Seglen and Gordon, 1982; Xu *et al.*, 2007). Somewhat to our surprise, although 3-MA (10 mM) itself did not affect autophagy, the PI3K inhibitor further exaggerated lethal toxin-induced autophagosome formation (GFP–LC3^{+} puncta) without affecting the lethal toxin-induced up-regulation in Beclin-1 and LC3-II-to-LC3-I ratio. Pretreatment with the autophagy inhibitor 3-MA (10 mM) for 24 h down-regulated the expression of PI3K and this effect was unaffected by lethal toxin exposure. PI3K knockdown using siRNA significantly inhibit lethal toxin-induced autophagosome formation as evidenced by the LC3-II-to-LC3-I ratio. PI3K knockdown itself did not affect the LC3-II-to-LC3-I ratio (Figure 7).

ER stress is not involved in lethal toxin-induced autophagy

ER stress is known to trigger autophagy (Yorimitsu *et al.*, 2006). Hence, we investigated the effect of lethal toxin exposure on ER stress. Expression of the ER stress markers BiP, calreticulin and eIF2α phosphorylation was assessed in H9C2 cells following lethal toxin exposure. Lethal toxin reduced the levels of Bip, although it failed to alter calreticulin expression and phosphorylation of eIF2α. Similarly, *in vivo* lethal toxin exposure (2 μg·g^{-1}, i.p., 18 h) failed to affect the expression of BiP and calreticulin as well as phosphorylation of eIF2α in WT or TLR4 knockout murine hearts (Figure 8).

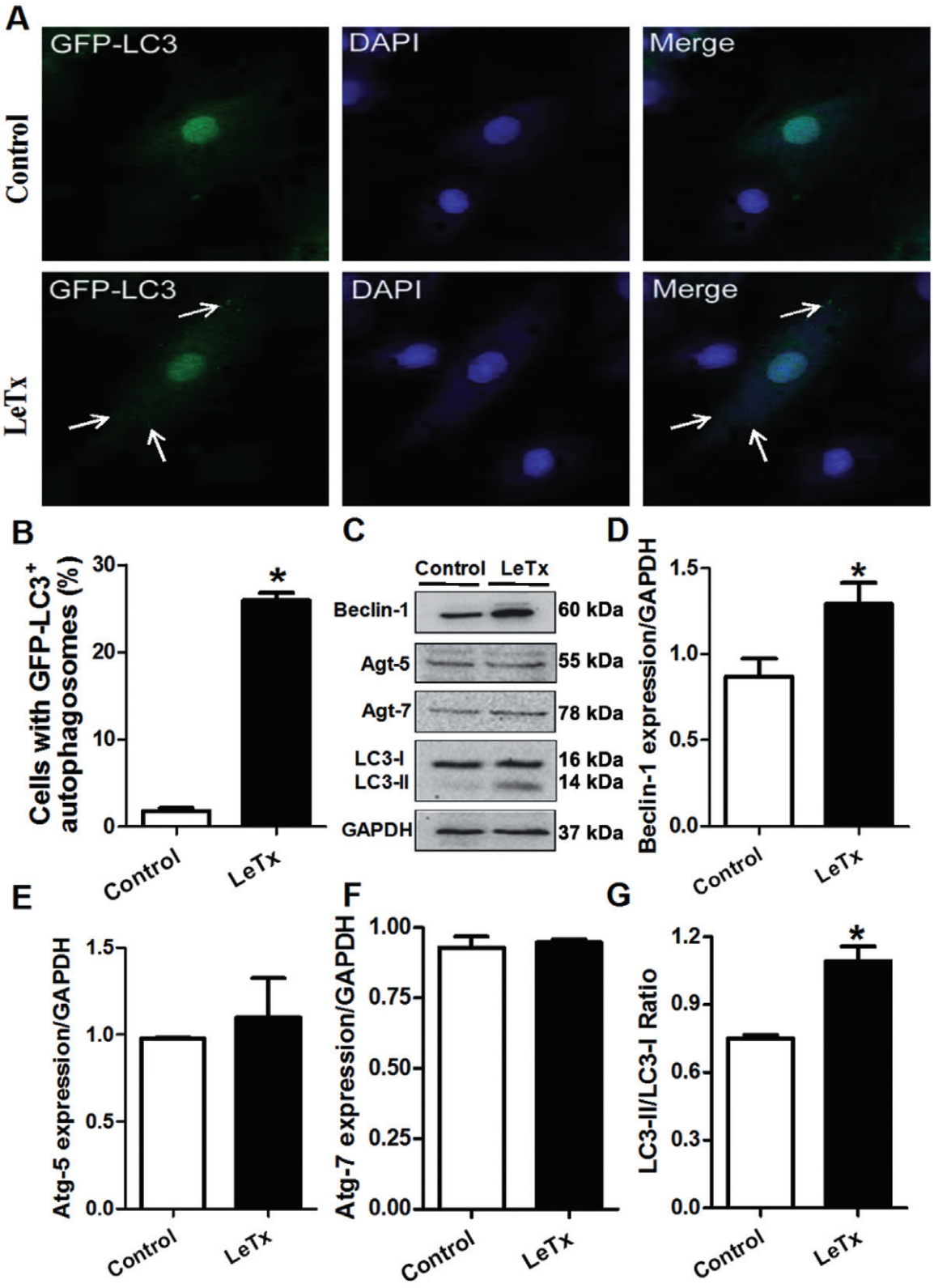

Figure 5

Effect of LeTx (100 ng·mL^{-1} for 3 h) on autophagy in cultured H9C2 cells. (A) Representative fluorescent images of GFP-LC-3II (puncta shown in arrowheads). (B) Quantification of cells with GFP–LC3^{+} autophagosomes. (C) Representative gel blots depicting expression of Beclin-1, Atg5, Atg7, LC-3 and GAPDH (loading control) in control and LeTx-treated cells. (D) Beclin-1. (E) Atg5. (F) Atg7. (G) LC3-II/LC3-I ratio. Mean ± SEM, $n = 3$ independent cultures, *$P < 0.05$ versus control group.

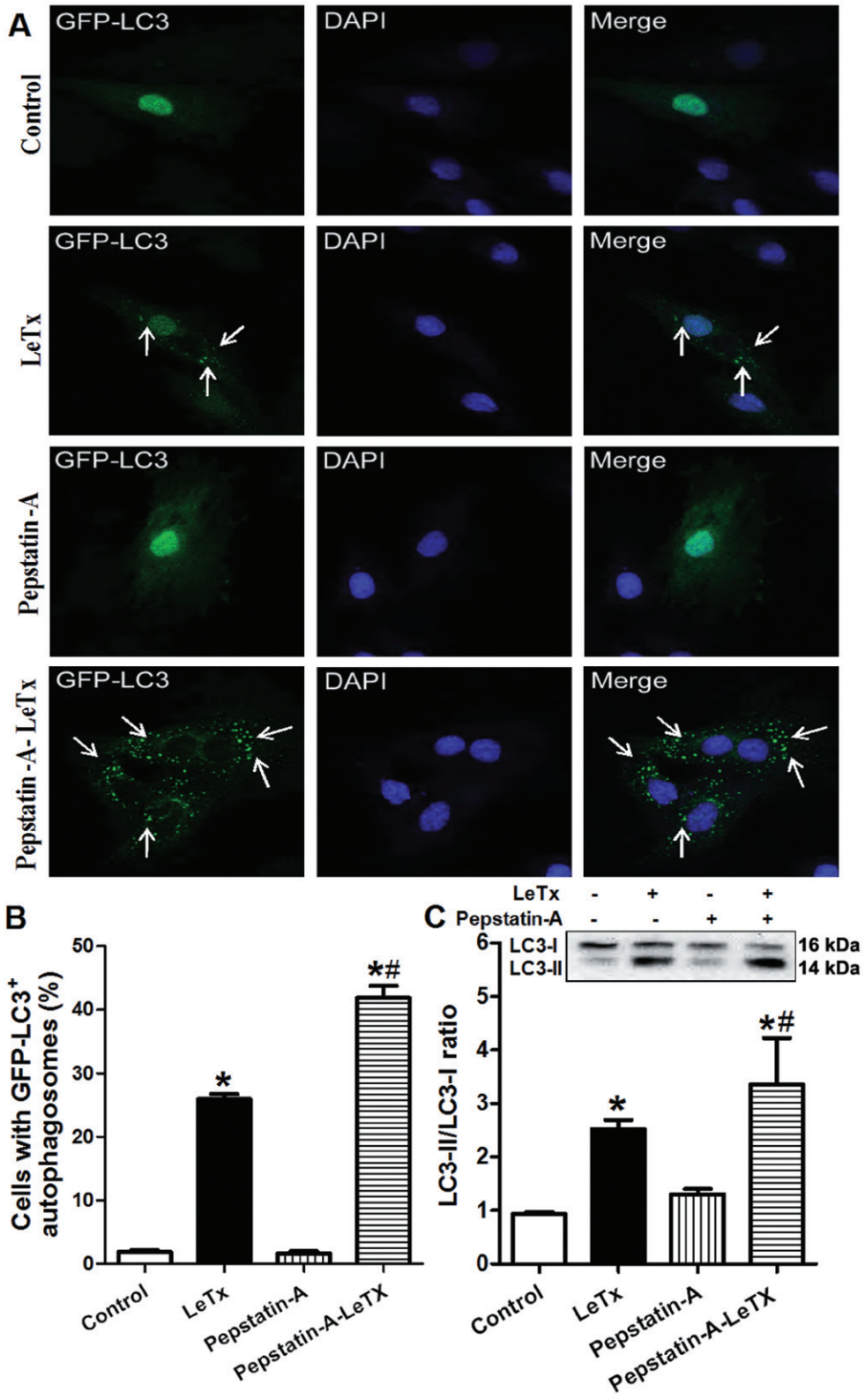

Figure 6

LeTx (100 ng·mL^{-1} for 3 h)-induced autophagy in H9C2 cells in the absence or presence of the lysosomal inhibitor pepstatin-A. (A) Representative microscopic images of GFP-LC3II (puncta shown in arrowheads). (B) Quantitation of cells with autophagosomes. (C) LC3-II/LC3-I ratio. Inset: Representative gel blots depicting expression of LC3 and GAPDH (loading control). Mean ± SEM, $n = 3$ independent cultures, *$P < 0.05$ versus control group, #$P < 0.05$ versus LeTx group.

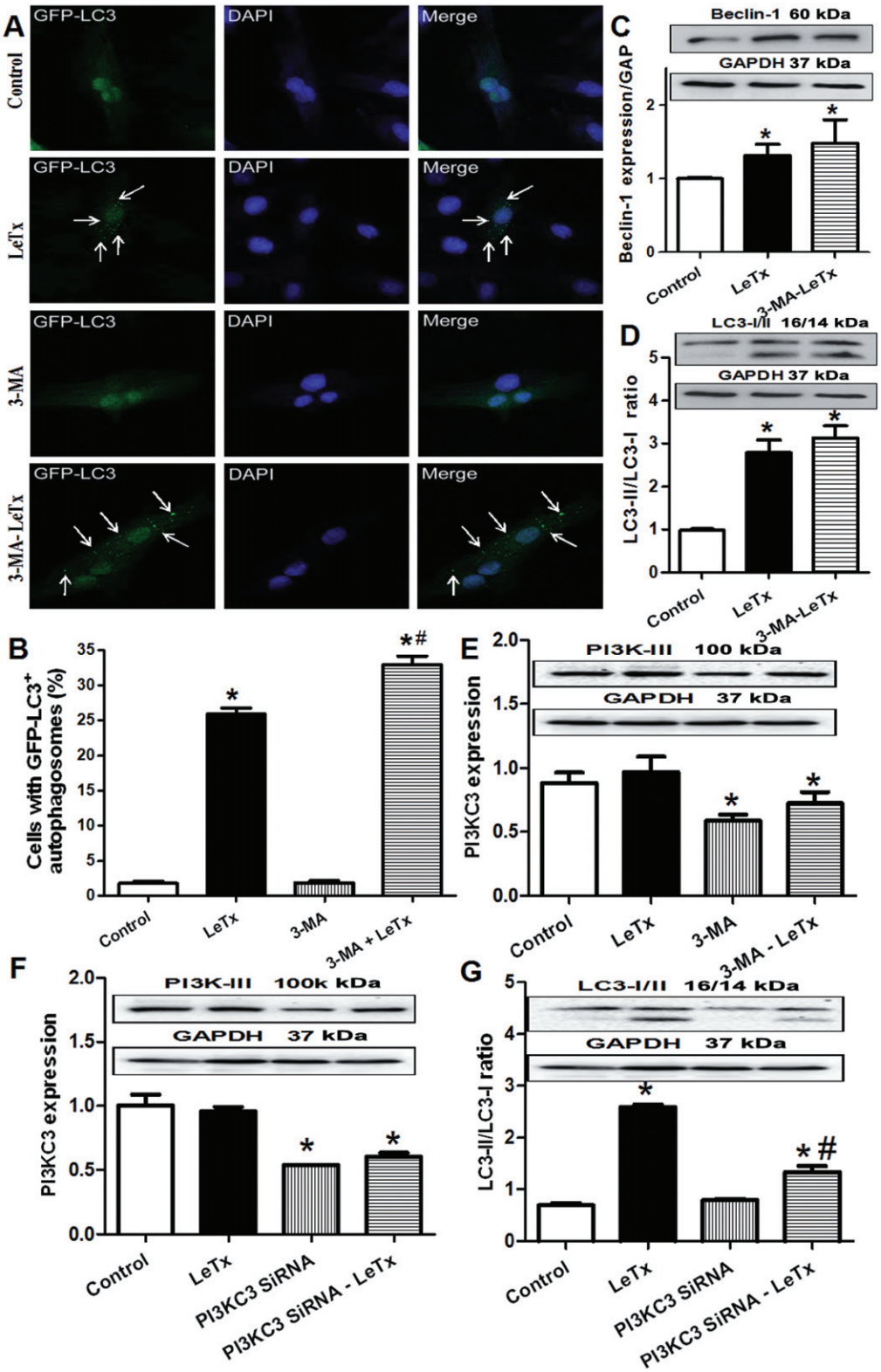

Figure 7

(A–E) Effect of class III PI3K inhibition using 3-MA (10 mM for 24 h) on LeTx (100 ng·mL^{-1} for 3 h)-induced autophagy in H9C2 cells. (A) Representative fluorescent images of GFP–LC3II (puncta shown in arrowheads). (B) Quantification of cells with GFP–LC3^{+} autophagosomes. (C) Beclin-1. (D) LC3-II/LC3-I ratio. (E) PI3K class III. (F–G) Effect of class III PI3K knockdown using siRNA on LeTx (100 ng·mL^{-1} for 3 h)-induced autophagy in H9C2 cells. (F) PI3K class III. (G) LC3-II/LC3-I ratio. Insets: representative gel blots depicting levels of Beclin-1, LC3, PI3K class III and GAPDH (loading control). Mean ± SEM, n = 3 independent cultures, *P < 0.05 versus control group; #P < 0.05 versus LeTx group.

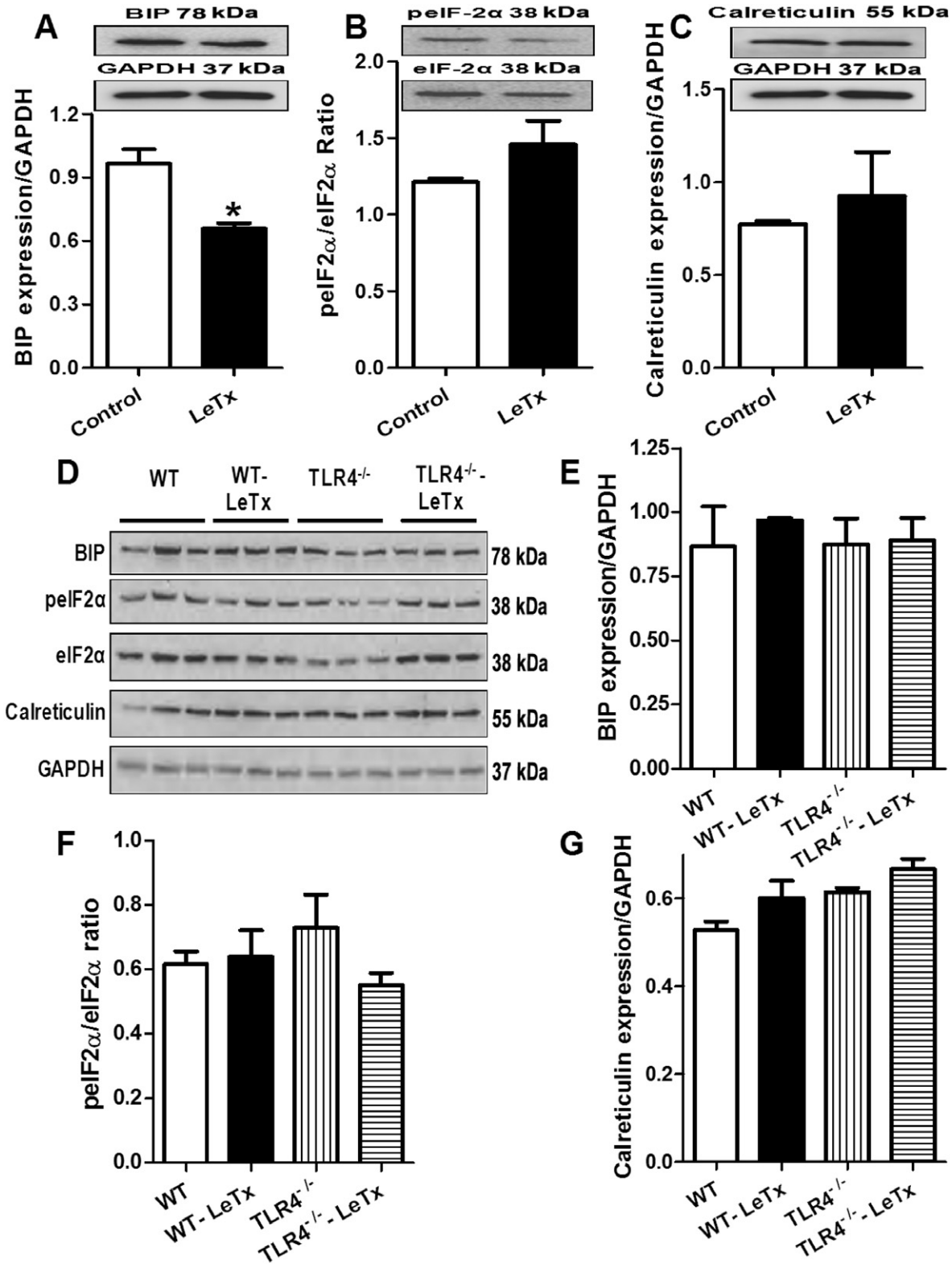

Figure 8

Effect of TLR4 knockout on LeTx-induced changes in ER stress. (A–C) Effect of *in vitro* LeTx exposure (100 ng·mL^{-1}, for 3 h) on the ER stress markers BiP, p-eIF2α to eIF2α ratio and calreticulin in cultured H9C2 cells. Insets: representative gel blots depicting expression of BiP, p-eIF2α, eIF2α, calreticulin and GAPDH (loading control). (D) Representative gel blots depicting expression of Bip, p-eIF2α, eIF2α, calreticulin and GAPDH (loading control) in myocardium from WT and TLR4$^{-/-}$ mice challenged with or without LeTx (2 μg·g^{-1}, i.p., 18 h). (E) BiP. (F) p-eIF2α to eIF2α ratio. (G) Calreticulin. Mean ± SEM, n = 4–6 mice or cultures per group, *P < 0.05 versus control group.

Discussion

The salient findings from our study reveal that knockout of the TLR4 receptor prevents lethal toxin-induced cardiac contractile and intracellular Ca^{2+} anomalies. The TLR4 knockout-induced cardioprotection against lethal toxin was associated with reduced autophagy induction. The findings from our *in vitro* experiments further confirmed the causative role of autophagy in lethal toxin- and TLR4 knockout-induced cardiac contractile responses.

There is ample experimental evidence for the devastating cardiac sequelae that follow anthrax exposure (Borio *et al.*, 2001; Mina *et al.*, 2002; Hsu *et al.*, 2004; Watson *et al.*, 2007a; Kuo *et al.*, 2008; Lawrence *et al.*, 2009; Moayeri *et al.*, 2009; Sweeney *et al.*, 2010). The findings from our study revealed that anthrax lethal toxin significantly decreases fractional shortening and cardiac output associated with reduced EDD as well as unchanged wall thickness and ESD. Indeed, anthrax lethal toxin was recently reported to significantly decrease heart rate, coronary flow, left ventricular developed pressure, rate-pressure product and dP/dt_{max} resulting in overt myocardial depression (Hicks *et al.*, 2011). The reduced cardiac output and LVEDD following lethal toxin challenge may be the result of impaired diastolic filling, which is consistent with the prolonged diastolic duration (TR_{90}). Although haemodynamic factors (such as changes in preload and afterload) may contribute to anthrax lethal toxin-induced changes in cardiac function, the fact that TLR4 knockout prevented this lethal toxin-induced decrease in cardiomyocyte contractile capacity suggests that this beneficial cardiac effect induced by TLR4 knockout is likely to originate from the heart as opposed to systemic circulatory factors. Nonetheless, further studies are needed to elucidate the lethal toxin-induced changes in diastolic function. The findings from our current study also revealed that lethal toxin inhibits cardiomyocyte contractile and intracellular Ca^{2+} properties. Depressed PS and $\pm dL/dt$, TR_{90} are in line with a reduction in the stimulated intracellular Ca^{2+} rise (ΔFFI) and slowed intracellular Ca^{2+} decay. These results accord with data obtained in our recent report (Kandadi *et al.*, 2010). The lethal toxin-induced cardiac contractile and intracellular Ca^{2+} derangements were significantly attenuated or prevented by TLR4 knockout. Lethal toxin exposure failed to alter the expression (or phosphorylation) of the key intracellular Ca^{2+} regulatory proteins SERCA2a and phospholamban, consistent with previous findings (Kandadi *et al.*, 2010). The observation that TLR4 knockout significantly ameliorated lethal toxin-induced cardiac dysfunction, intracellular Ca^{2+} dysregulation and autophagy favours a role for autophagy and intracellular Ca^{2+} handling in lethal toxin- and TLR4 knockout-elicited cardiac responses.

One of the most intriguing data from our study is that anthrax lethal toxin exposure induced overt myocardial autophagy, the effect of which was attenuated or prevented by TLR4 knockout. Similarly, a reversal of lethal toxin-induced LC3-II expression was noted in the TLR4- or class III PI3K-knockdown groups in the *in vitro* setting. Enhanced autophagy is observed in the failing heart in a wide array of cardiovascular diseases resulting in cardiac cell death and impaired cardiac performance (Knaapen *et al.*, 2001; Shimomura *et al.*, 2001; Kostin *et al.*, 2003). Thus attenuation of autophagy by TLR4 knockout or knockdown corroborates the TLR4 knockout- or deficiency-triggered resistance against anthrax spore challenge (Hsu *et al.*, 2004; Hughes *et al.*, 2005). TLR4 regulates autophagy via a Toll–IL-1 receptor domain-containing adaptor-inducing IFN-β (TRIF)-dependent, myeloid differentiating factor 88 (MyD88)-independent TLR4 signalling pathway (Xu *et al.*, 2007). Autophagy starts with an induction phase that can be initiated by kinase complex that consists of class III PI3K, p150 myristylated protein kinase and beclin-1. Although knockdown of class III PI3K attenuated lethal toxin-induced rise in LC3II-to-LC3I ratio, our *in vitro* data using the PI3-kinase inhibitor 3-MA failed to inhibit lethal toxin-induced autophagy. The discrepancy between the class III PI3K siRNA and 3-MA is still unknown, although it may be related to a possible non-specific effect of 3-MA. To-date, the precise mechanism behind lethal toxin-induced autophagy still remains elusive. During the delayed phase in autophagosome formation, the autophagosome membrane elongates and this involves several autophagy proteins such as Atg5, Atg12, Atg7 and the autophagosomal membrane specific protein light chain 3 (LC3) (i.e. Atg8). Autophagosome fuses with lysosome forming autolysosome before being degraded by lysosomal proteases (He and Klionsky, 2009; Tang *et al.*, 2009). Data from our present study showed an increased conversion of LC3-I to LC3-II, an important step for autophagosome formation. However, to our surprise, there was little change in the expression of Atg5 and Atg7. One possible explanation for this discrepant finding may be the involvement of an Atg5/Atg7-independent alternative pathway of autophagy following lethal toxin exposure (Nishida *et al.*, 2009). In addition, based on the findings obtained with the lysosomal enzyme inhibitor, the increase in LC3-II expression levels may be the result of enhanced autophagic flux following lethal toxin exposure.

The ER is an extensive intracellular membranous network involved in Ca^{2+} storage, Ca^{2+} signalling, glycosylation and trafficking of membrane and secretory proteins. In stress conditions, the three distinct classes of ER stress transducers IRE1, PERK/eIF2α and activating transcription factor 6 (ATF6) mediate unfolded protein response (UPR) (Ron and Walter, 2007). It has been reported that ER stress induces autophagy via eIF2α phosphorylation during starvation conditions and viral infections (Talloczy *et al.*, 2002). Data from our study revealed little change in the ER stress markers following exposure to the anthrax lethal toxin. In fact, a decrease in the expression of BiP was noted following lethal toxin challenge. BiP is an ER chaperone (also known as GRP78) that interacts with all three ER stress sensors PERK/eIF2α, ATF6 and IRE1. *In vivo* anthrax lethal toxin exposure failed to alter eIF2α phosphorylation, or BiP and calreticulin expression. Taken together, our results do not support a role for ER stress in anthrax lethal toxin-induced cardiac contractile anomalies. Recent findings from our laboratory indicated that lethal toxin may interrupt cardiac contractile function and intracellular Ca^{2+} homeostasis through accumulation of reactive oxygen species via a NADPH oxidase-dependent mechanism (Kandadi *et al.*, 2010). Along the same line, TLR4 has been shown to interact directly with NADPH oxidase *en route* to accumulation of reactive oxygen species (Asehnoune *et al.*, 2004; Park *et al.*, 2004). It is possible that TLR4 knockout may

protect cardiac contractile dysfunction by removing NADPH oxidase-dependent oxidative stress. Recent evidence from our laboratory further revealed that the antioxidant enzyme catalase protects against anthrax lethal toxin-induced cardiac dysfunction (Kandadi and Ren, unpublished data). However, a further study is warranted to examine the role of NADPH oxidase in the management of anthrax lethal toxin-induced cardiac anomalies.

In conclusion, the findings from our present study reveal that TLR4 knockout provides effective cardioprotection against anthrax lethal toxin. TLR4 knockout prevents lethal toxin-induced cardiac contractile and intracellular Ca^{2+} anomalies, possibly through a mechanism associated with autophagy. These findings suggest that compounds that negatively modulate TLR4 signalling and autophagy could be used in the therapeutics and management of anthrax infection-induced cardiovascular complications.

Acknowledgements

This work was supported in part by NIH/NCRR P20 RR016474. None of the authors declares any conflicts of interest.

Conflict of interest

None.

References

Asehnoune K, Strassheim D, Mitra S, Kim JY, Abraham E (2004). Involvement of reactive oxygen species in Toll-like receptor 4-dependent activation of NF-kappa B. J Immunol 172: 2522–2529.

Barakat LA, Quentzel HL, Jernigan JA, Kirschke DL, Griffith K, Spear SM *et al.* (2002). Fatal inhalational anthrax in a 94-year-old Connecticut woman. JAMA 287: 863–868.

Baumgarten G, Knuefermann P, Nozaki N, Sivasubramanian N, Mann DL, Vallejo JG (2001). In vivo expression of proinflammatory mediators in the adult heart after endotoxin administration: the role of toll-like receptor-4. J Infect Dis 183: 1617–1624.

Borio L, Frank D, Mani V, Chiriboga C, Pollanen M, Ripple M *et al.* (2001). Death due to bioterrorism-related inhalational anthrax: report of 2 patients. JAMA 286: 2554–2559.

Bradley KA, Mogridge J, Mourez M, Collier RJ, Young JA (2001). Identification of the cellular receptor for anthrax toxin. Nature 414: 225–229.

Ceylan-Isik AF, Guo KK, Carlson EC, Privratsky JR, Liao SJ, Cai L *et al.* (2009). Metallothionein abrogates GTP cyclohydrolase I inhibition-induced cardiac contractile and morphological defects: role of mitochondrial biogenesis. Hypertension 53: 1023–1031.

Cui X, Moayeri M, Li Y, Li X, Haley M, Fitz Y *et al.* (2004). Lethality during continuous anthrax lethal toxin infusion is associated with circulatory shock but not inflammatory cytokine or nitric oxide release in rats. Am J Physiol Regul Integr Comp Physiol 286: R699–R709.

Dong F, Zhang X, Wold LE, Ren Q, Zhang Z, Ren J (2005). Endothelin-1 enhances oxidative stress, cell proliferation and reduces apoptosis in human umbilical vein endothelial cells: role of ETB receptor, NADPH oxidase and caveolin-1. Br J Pharmacol 145: 323–333.

Edick MJ, Tesfay L, Lamb LE, Knudsen BS, Miranti CK (2007). Inhibition of integrin-mediated crosstalk with epidermal growth factor receptor/Erk or Src signaling pathways in autophagic prostate epithelial cells induces caspase-independent death. Mol Biol Cell 18: 2481–2490.

Fraser CM, Dando MR (2001). Genomics and future biological weapons: the need for preventive action by the biomedical community. Nat Genet 29: 253–256.

Gardin JM, Siri FM, Kitsis RN, Edwards JG, Leinwand LA (1995). Echocardiographic assessment of left ventricular mass and systolic function in mice. Circ Res 76: 907–914.

He C, Klionsky DJ (2009). Regulation mechanisms and signaling pathways of autophagy. Annu Rev Genet 43: 67–93.

Hicks CW, Li Y, Okugawa S, Solomon SB, Moayeri M, Leppla SH *et al.* (2011). Anthrax edema toxin has cAMP-mediated stimulatory effects and high-dose lethal toxin has depressant effects in an isolated perfused rat heart model. Am J Physiol Heart Circ Physiol 300: H1108–H1118.

Hintz KK, Relling DP, Saari JT, Borgerding AJ, Duan J, Ren BH *et al.* (2003). Cardiac overexpression of alcohol dehydrogenase exacerbates cardiac contractile dysfunction, lipid peroxidation, and protein damage after chronic ethanol ingestion. Alcohol Clin Exp Res 27: 1090–1098.

Hsu LC, Park JM, Zhang K, Luo JL, Maeda S, Kaufman RJ *et al.* (2004). The protein kinase PKR is required for macrophage apoptosis after activation of Toll-like receptor 4. Nature 428: 341–345.

Hughes MA, Green CS, Lowchyj L, Lee GM, Grippe VK, Smith MF Jr *et al.* (2005). MyD88-dependent signaling contributes to protection following Bacillus anthracis spore challenge of mice: implications for Toll-like receptor signaling. Infect Immun 73: 7535–7540.

Kabeya Y, Mizushima N, Ueno T, Yamamoto A, Kirisako T, Noda T *et al.* (2000). LC3, a mammalian homologue of yeast Apg8p, is localized in autophagosome membranes after processing. EMBO J 19: 5720–5728.

Kandadi MR, Hua Y, Ma H, Li Q, Kuo SR, Frankel AE *et al.* (2010). Anthrax lethal toxin suppresses murine cardiomyocyte contractile function and intracellular Ca2+ handling via a NADPH oxidase-dependent mechanism. PLoS ONE 5: e13335.

Kilkenny C, Browne W, Cuthill IC, Emerson M, Altman DG (2010). NC3Rs Reporting Guidelines Working Group. Br J Pharmacol 160: 1577–1579.

Knaapen MW, Davies MJ, De Bie M, Haven AJ, Martinet W, Kockx MM (2001). Apoptotic versus autophagic cell death in heart failure. Cardiovasc Res 51: 304–312.

Kostin S, Pool L, Elsasser A, Hein S, Drexler HC, Arnon E *et al.* (2003). Myocytes die by multiple mechanisms in failing human hearts. Circ Res 92: 715–724.

Kroemer G, Marino G, Levine B (2010). Autophagy and the integrated stress response. Mol Cell 40: 280–293.

Kuo SR, Willingham MC, Bour SH, Andreas EA, Park SK, Jackson C *et al.* (2008). Anthrax toxin-induced shock in rats is associated with pulmonary edema and hemorrhage. Microb Pathog 44: 467–472.

Lawrence WS, Hardcastle JM, Brining DL, Weaver LE, Ponce C, Whorton EB *et al*. (2009). The physiologic responses of Dutch belted rabbits infected with inhalational anthrax. Comp Med 59: 257–265.

McGrath J, Drummond G, McLachlan E, Kilkenny C, Wainwright C (2010). Guidelines for reporting experiments involving animals: the ARRIVE guidelines. Br J Pharmacol 160: 1573–1576.

Mina B, Dym JP, Kuepper F, Tso R, Arrastia C, Kaplounova I *et al*. (2002). Fatal inhalational anthrax with unknown source of exposure in a 61-year-old woman in New York City. JAMA 287: 858–862.

Moayeri M, Leppla SH (2009). Cellular and systemic effects of anthrax lethal toxin and edema toxin. Mol Aspects Med 30: 439–455.

Moayeri M, Martinez NW, Wiggins J, Young HA, Leppla SH (2004). Mouse susceptibility to anthrax lethal toxin is influenced by genetic factors in addition to those controlling macrophage sensitivity. Infect Immun 72: 4439–4447.

Moayeri M, Crown D, Dorward DW, Gardner D, Ward JM, Li Y *et al*. (2009). The heart is an early target of anthrax lethal toxin in mice: a protective role for neuronal nitric oxide synthase (nNOS). PLoS Pathog 5: e1000456.

Nishida Y, Arakawa S, Fujitani K, Yamaguchi H, Mizuta T, Kanaseki T *et al*. (2009). Discovery of Atg5/Atg7-independent alternative macroautophagy. Nature 461: 654–658.

Park HS, Jung HY, Park EY, Kim J, Lee WJ, Bae YS (2004). Cutting edge: direct interaction of TLR4 with NAD(P)H oxidase 4 isozyme is essential for lipopolysaccharide-induced production of reactive oxygen species and activation of NF-kappa B. J Immunol 173: 3589–3593.

Poltorak A, He X, Smirnova I, Liu MY, Van Huffel C, Du X *et al*. (1998). Defective LPS signaling in C3H/HeJ and C57BL/10ScCr mice: mutations in Tlr4 gene. Science 282: 2085–2088.

Relling DP, Hintz KK, Ren J (2003). Acute exposure of ceramide enhances cardiac contractile function in isolated ventricular myocytes. Br J Pharmacol 140: 1163–1168.

Ron D, Walter P (2007). Signal integration in the endoplasmic reticulum unfolded protein response. Nat Rev Mol Cell Biol 8: 519–529.

Rossi CA, Ulrich M, Norris S, Reed DS, Pitt LM, Leffel EK (2008). Identification of a surrogate marker for infection in the African green monkey model of inhalation anthrax. Infect Immun 76: 5790–5801.

Schwandner R, Dziarski R, Wesche H, Rothe M, Kirschning CJ (1999). Peptidoglycan- and lipoteichoic acid-induced cell activation is mediated by toll-like receptor 2. J Biol Chem 274: 17406–17409.

Scobie HM, Rainey GJ, Bradley KA, Young JA (2003). Human capillary morphogenesis protein 2 functions as an anthrax toxin receptor. Proc Natl Acad Sci U S A 100: 5170–5174.

Seglen PO, Gordon PB (1982). 3-Methyladenine: specific inhibitor of autophagic/lysosomal protein degradation in isolated rat hepatocytes. Proc Natl Acad Sci U S A 79: 1889–1892.

Shimomura H, Terasaki F, Hayashi T, Kitaura Y, Isomura T, Suma H (2001). Autophagic degeneration as a possible mechanism of myocardial cell death in dilated cardiomyopathy. Jpn Circ J 65: 965–968.

Sweeney DA, Cui X, Solomon SB, Vitberg DA, Migone TS, Scher D *et al*. (2010). Anthrax lethal and edema toxins produce different patterns of cardiovascular and renal dysfunction and synergistically decrease survival in canines. J Infect Dis 202: 1885–1896.

Takeda K, Akira S (2005). Toll-like receptors in innate immunity. Int Immunol 17: 1–14.

Talloczy Z, Jiang W, Virgin HW, Leib DA, Scheuner D, Kaufman RJ *et al*. (2002). Regulation of starvation- and virus-induced autophagy by the eIF2alpha kinase signaling pathway. Proc Natl Acad Sci U S A 99: 190–195.

Tang S, Moayeri M, Chen Z, Harma H, Zhao J, Hu H *et al*. (2009). Detection of anthrax toxin by an ultrasensitive immunoassay using europium nanoparticles. Clin Vaccine Immunol 16: 408–413.

Tanida I, Minematsu-Ikeguchi N, Ueno T, Kominami E (2005). Lysosomal turnover, but not a cellular level, of endogenous LC3 is a marker for autophagy. Autophagy 1: 84–91.

Watson LE, Kuo SR, Katki K, Dang T, Park SK, Dostal DE *et al*. (2007a). Anthrax toxins induce shock in rats by depressed cardiac ventricular function. PLoS ONE 2: e466.

Watson LE, Mock J, Lal H, Lu G, Bourdeau RW, Tang WJ *et al*. (2007b). Lethal and edema toxins of anthrax induce distinct hemodynamic dysfunction. Front Biosci 12: 4670–4675.

Xu Y, Jagannath C, Liu XD, Sharafkhaneh A, Kolodziejska KE, Eissa NT (2007). Toll-like receptor 4 is a sensor for autophagy associated with innate immunity. Immunity 27: 135–144.

Yorimitsu T, Nair U, Yang Z, Klionsky DJ (2006). Endoplasmic reticulum stress triggers autophagy. J Biol Chem 281: 30299–30304.